Supplementary Information

Hydroxyethyl cellulose optimized cathode/electrolyte interfaces in aqueous zinc ion batteries

Sheng Lu[a], Yuyang Gu[b], Guangyu Cheng[b], Yueni Mei[b], Dongqing Wu[, c], Yu Gao[a], Xuemin Yu[a], Liang Wu[c], Yuezeng Su[d], Han Wang*[, a]*

[a]School of Chemistry and Chemical Engineering, Shanghai University of Engineering Sciences, 333 Longteng Road, Shanghai, 201620 P. R. China. Email: wanghan@sues.edu.cn

[b]State Key Laboratory of Space Power-Sources, Shanghai Institute of Space Power-Sources, 2965 Dongchuan RD, Shanghai, 200245, China.

[c]School of Chemistry and Chemical Engineering, Shanghai Jiao Tong University, 800 Dongchuan Road, Shanghai, 200240 P. R. China. Email: wudongqing@sjtu.edu.cn

[d]School of Electronic Information and Electrical Engineering, Shanghai Jiao Tong University, 800 Dongchuan Road, Shanghai, 200240 P. R. China.

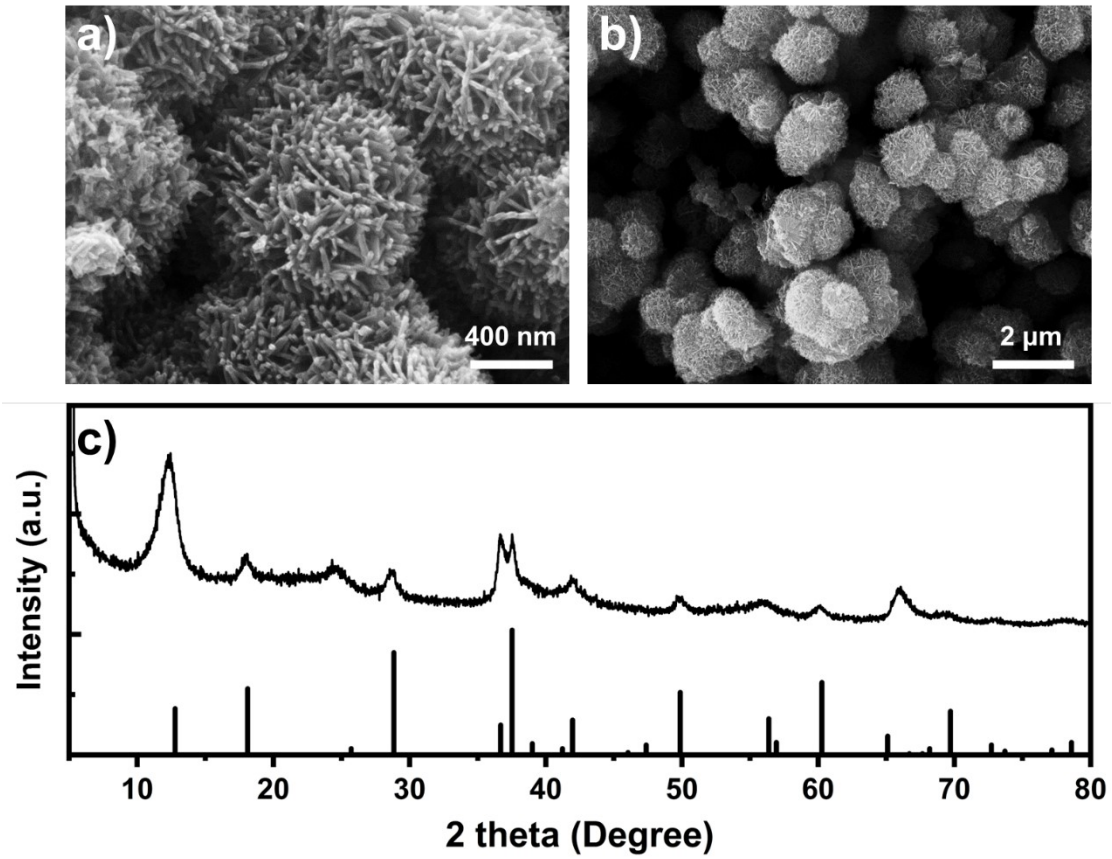

Figure S1 (a-b) SEM images of MnO_2 in different scales. (c) XRD patterns of MnO_2.

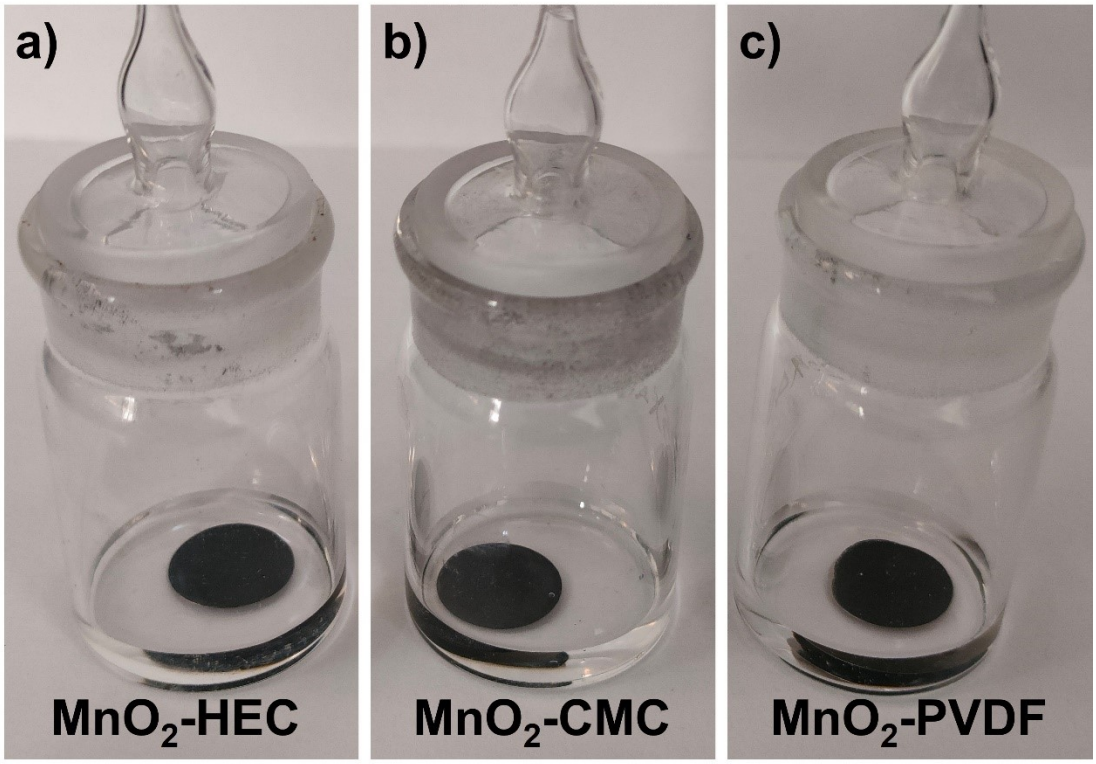

Figure S2 Digital photos of (a) MnO_2-HEC, (b) MnO_2-CMC, and (c) MnO_2-PVDF immersed in the aqueous electrolyte for a week.

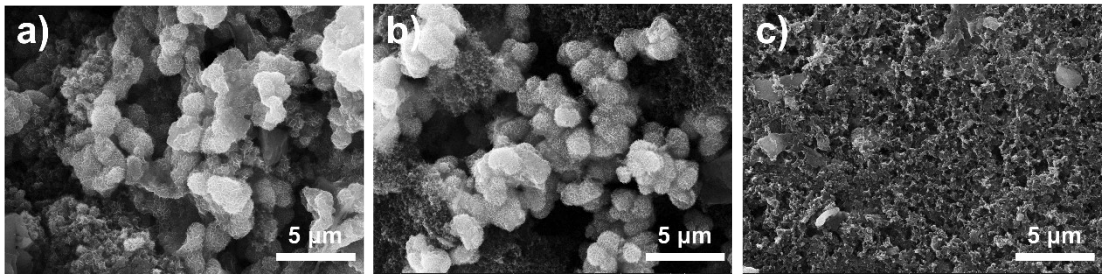

Figure S3 SEM images of (a) MnO_2-HEC, (b) MnO_2-CMC and (c) MnO_2-PVDF

Table S1. Fitting data of Nyquist plots in Figure 2a.

	MnO_2-HEC	MnO_2-CMC	MnO_2-PVDF
R_s (Ω)	1.41	1.64	1.83
CPE ($S \cdot sec^n \cdot cm^{-2}$)	0.00444	0.00671	0.00399
Freq power, n	0.71	0.90	0.97
R_{ct} (Ω)	133.50	141.00	1604.00
CPE ($S \cdot sec^n \cdot cm^{-2}$)	0.00032	0.00064	0.00059
Freq power, n	0.75	0.63	0.67
Warburg ($S \cdot sec^{0.5} \cdot cm^{-2}$)	0.00370	0.00133	0.00336

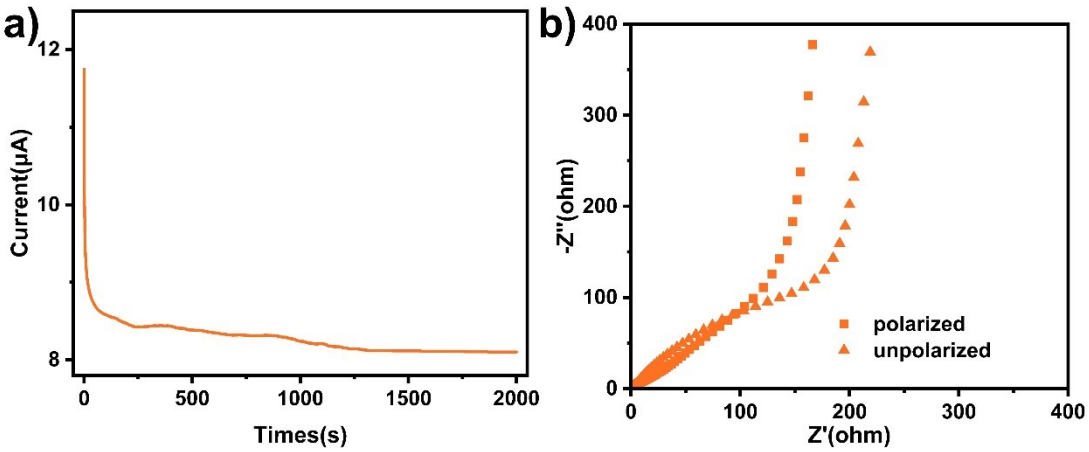

Figure S4 (a) Current-time plot of a Zn||MnO_2-HEC cell after the application of a constant potential (50 mV). (b) corresponding EIS data before and after polarization.

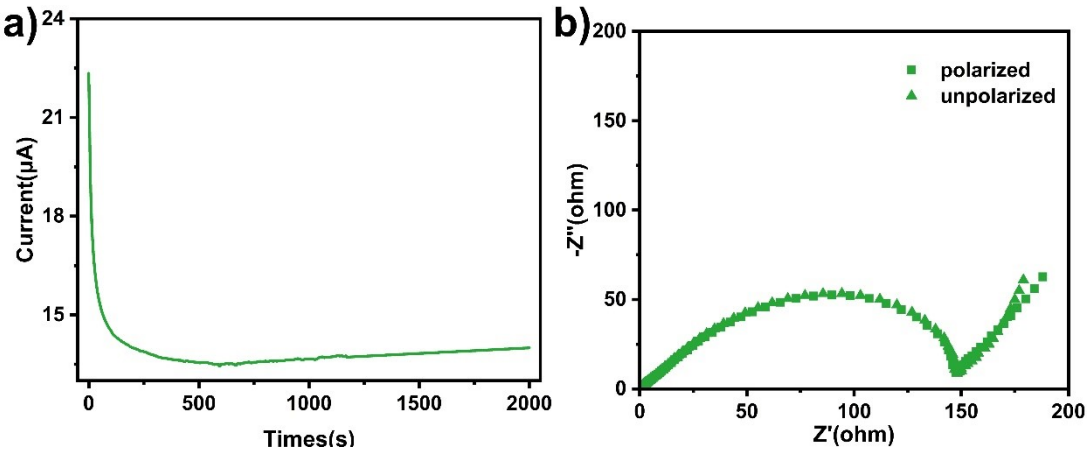

Figure S5 (a) Current-time plot of a Zn||MnO_2-CMC cell after the application of a constant potential (50 mV). (b) corresponding EIS data before and after polarization.

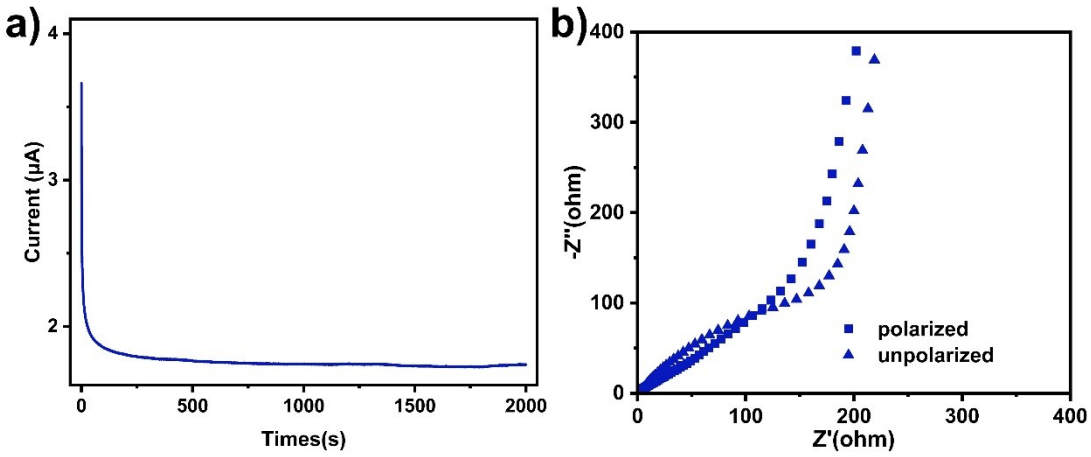

Figure S6 (a) Current-time plot of a Zn||MnO_2-PVDF cell after the application of a constant potential (50 mV). (b) corresponding EIS data before and after polarization.

Table S2 Specific parameters used to calculate t_{M^+}

Sample	I_{in} (A)	I_s (A)	R_{in} (Ω)	R_s (Ω)	Δv (V *vs.* Zn^{2+}/Zn)
MnO_2-PVDF	0.000003663	0.000001739	247.2	225.4	0.05
MnO_2-HEC	0.000011750	0.000008283	247.2	219.6	0.05
MnO_2-CMC	0.000022610	0.000014540	151.0	163.0	0.05

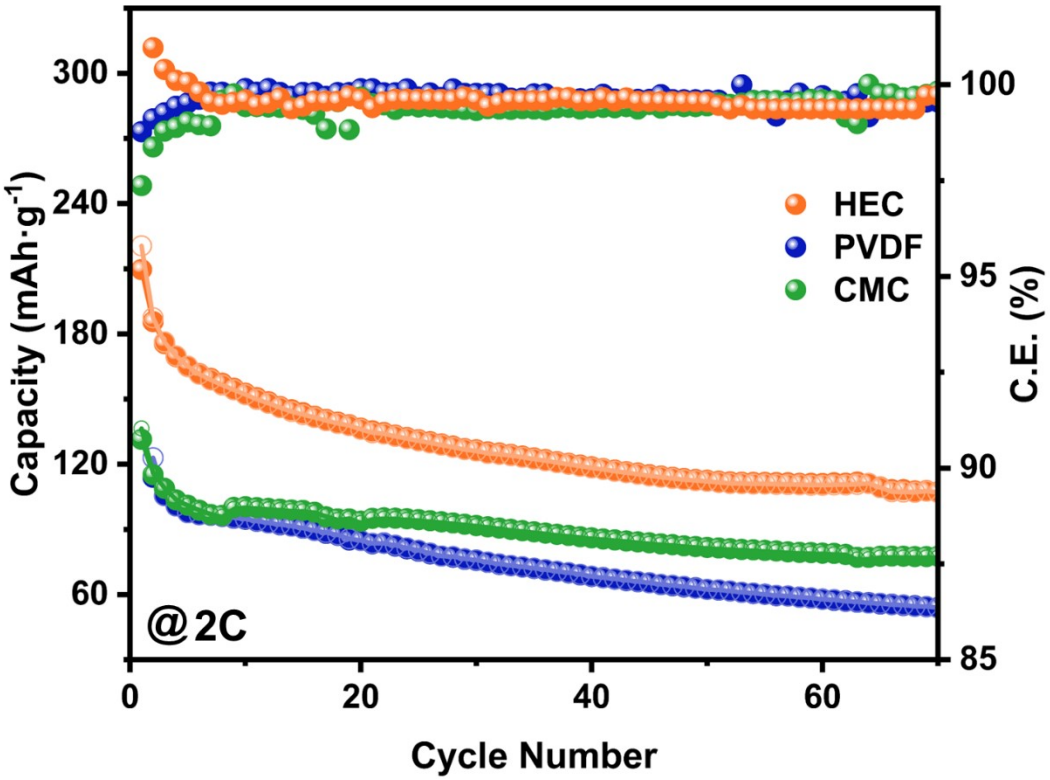

Figure S7 The cycling performances of the MnO_2-HEC, MnO_2-CMC and MnO_2-PVDF cells at 2C.

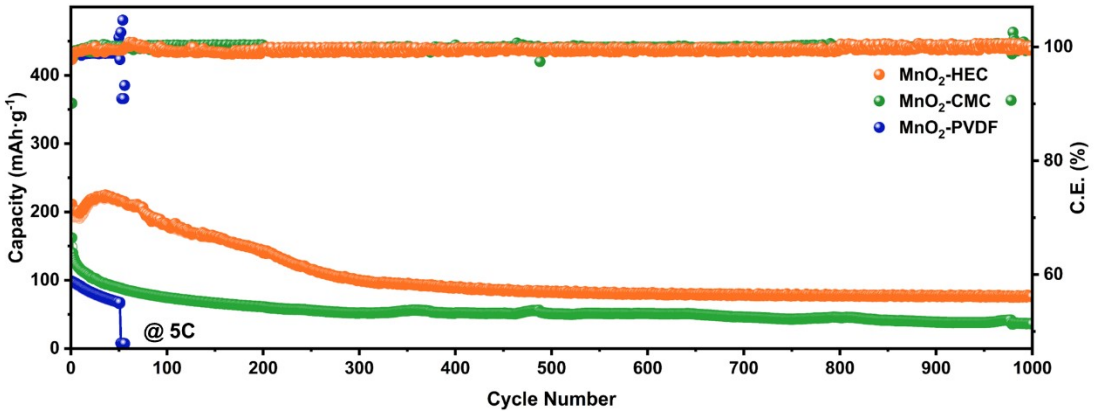

Figure S8 The cycling performances of the MnO_2-HEC, MnO_2-CMC and MnO_2-PVDF cells at 5C.

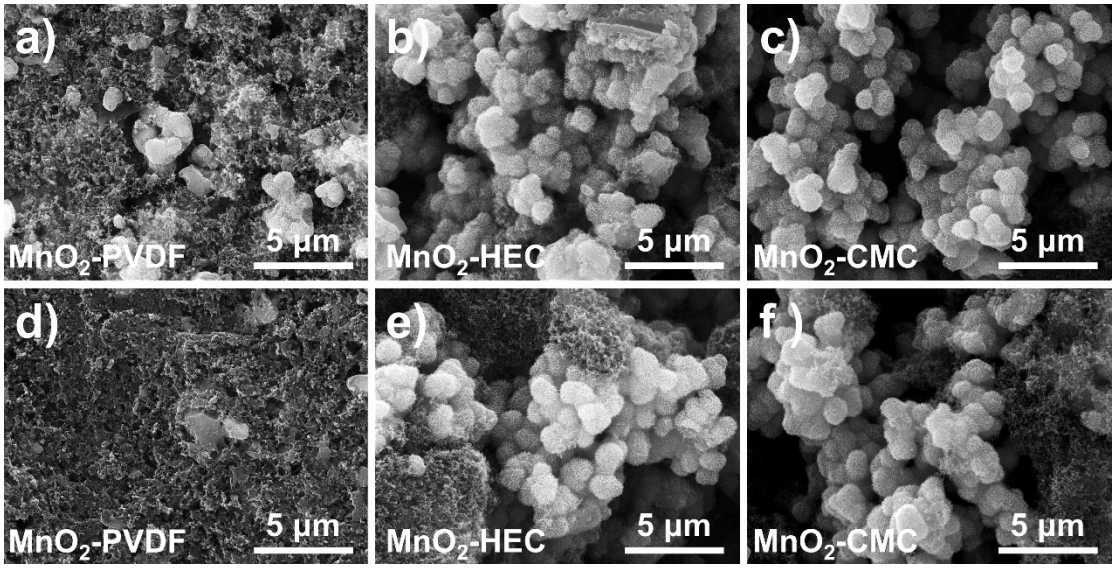

Figure S9 The SEM images of the cathodes with PVDF (a), HEC (b), CMC (c) as binders before cycling test. The SEM images of the cathodes with PVDF (d), HEC (e), CMC (f) as binders after 5 cycles at 5C.

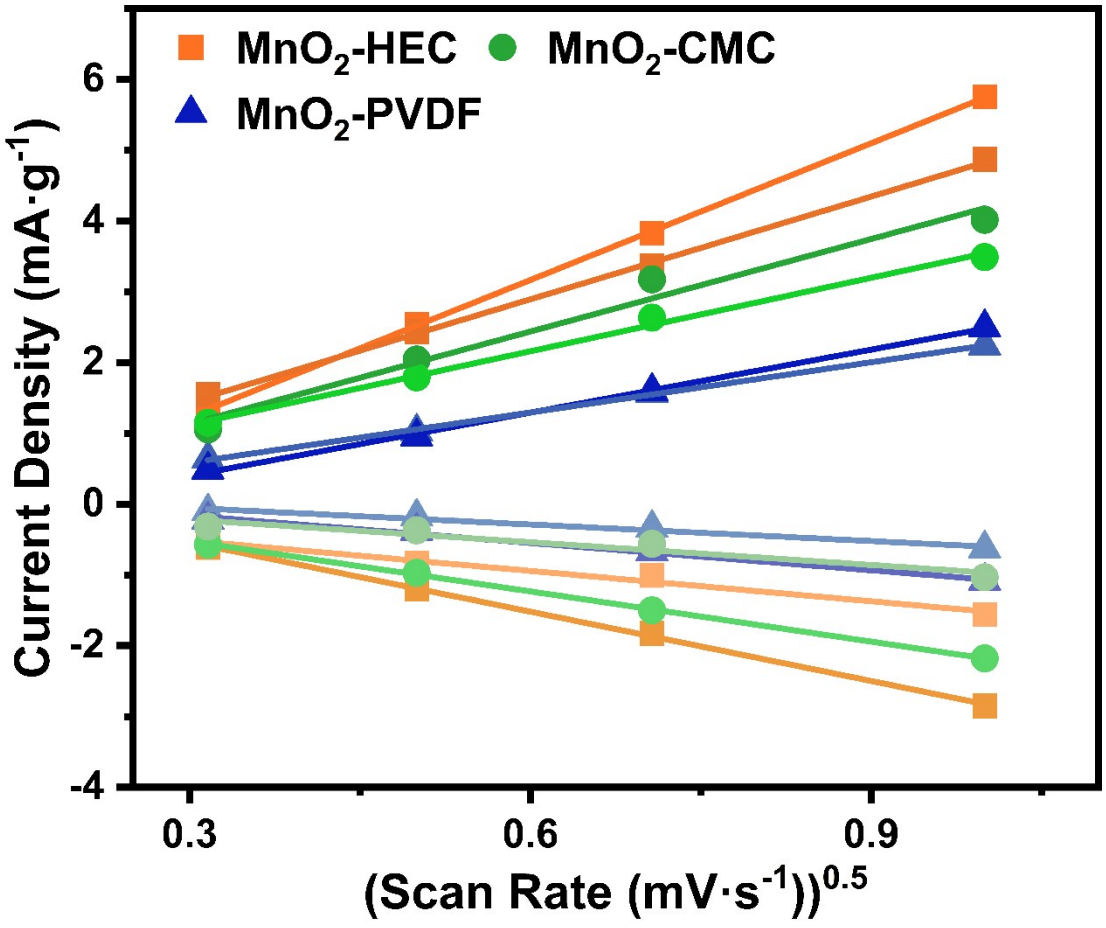

Figure S10 The calculated $D_{Zn^{2+}}$ of each peak for MnO_2-HEC, MnO_2-CMC, and MnO_2-PVDF.

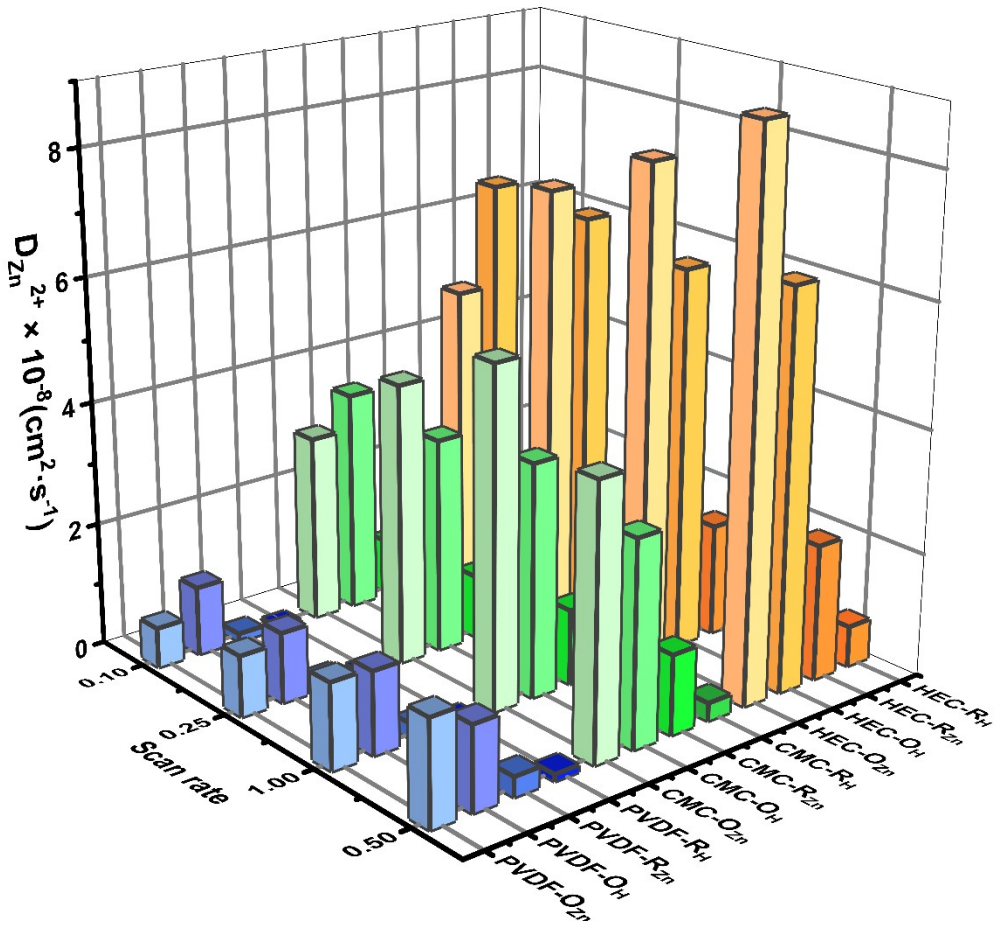

Figure S11 Diffusion coefficient of the MnO_2-HEC, MnO_2-CMC, and MnO_2-PVDF cells.

Table S3. Detailed data on the diffusion coefficient of the MnO_2-HEC, MnO_2-CMC, and MnO_2-PVDF cells.

Scan	MnO_2-HEC [a]				MnO_2-CMC [a]				MnO_2-PVDF [a]			
rate [b]	O_{Zn}	O_H	R_{Zn}	R_H	O_{Zn}	O_H	R_{Zn}	R_H	O_{Zn}	O_H	R_{Zn}	R_H
0.10	4.86	6.52	1.01	0.83	3.04	3.60	0.89	0.27	0.65	1.12	0.13	0.03
0.25	7.04	6.46	1.54	0.75	4.54	3.48	1.03	0.15	0.99	1.14	0.15	0.03
0.50	7.95	6.16	1.81	0.55	5.48	3.77	1.22	0.17	1.39	1.34	0.24	0.06
1.00	8.99	6.44	2.20	0.66	4.38	3.31	1.29	0.29	1.70	1.36	0.32	0.11

[a] The unit of diffusion coefficient is ($cm^2 \cdot S^{-1} \cdot 10^{-8}$). [b] The unit of scan rate is $mV \cdot s^{-1}$

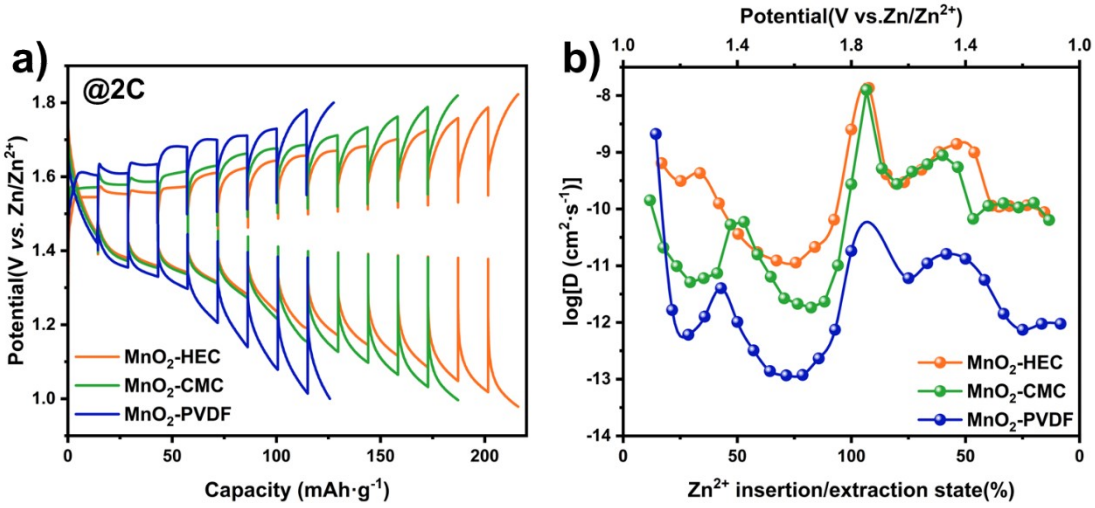

Figure S12 a) The GITT curves of the MnO_2-HEC, MnO_2-CMC, and MnO_2-PVDF cells at 2 C. b) Corresponding diffusion coefficients (*D*) of the cells.

Table S4. The performance comparasion of the MnO_2-HEC cell with those of the previously reported MnO_2-based AZIBs.

The types of binder	Energy Density ($Wh \cdot kg^{-1}$)	Power Density ($W \cdot kg^{-1}$)	Ref.
SA	370	555	1
PAN	279	72	2
	270	108	
	252	288	
	198	576	
	135	1152	
CMC	365.75	87.5	3
	218.75	175	
	192.5	350	
	140	700	
	105	1400	
CMC	194.4	2700	4
	518.4	180	
SA	234	54	5
	225	108	
	180	162	
	135	216	
	99	270	
	54	540	
	36	1080	
PEDOT:PSS	570	380	6
	235.6	1900	
	161.5	2850	
β-PVDF	512.45	185	7
	351.5	555	
	286.75	925	
	222	1850	
	166.5	3700	
	111	5550	
PAA	342	190	8
	298.3	380	
	281.2	570	
	273.6	760	
	231.8	1520	
	209	2280	
	163.4	4560	
	123.5	9120	

	618.66	108	
	487.62	270	
HEC	398.7	540	This Work
	332.1	1080	
	222.3	2700	

References

1. D. Xie, J. Zhao, Q. Jiang, H. Wang, H. Huang, P. Rao and J. Mao, *ChemPhysChem*, 2022, **23**, e202200106.
2. O. Fitz, S. Ingenhoven, C. Bischoff, H. Gentischer, K. P. Birke, D. Saracsan and D. Biro, *Batteries*, 2021, **7**, 40.
3. N. Jaikrajang, W. Kao-Ian, T. Muramatsu, R. Chanajaree, T. Yonezawa, Z. Y. Al Balushi, S. Kheawhom and R. Cheacharoen, *Acs Applied Energy Materials*, 2021, **4**, 7138-7147.
4. H. J. Chang, I. A. Rodríguez-Pérez, M. Fayette, N. L. Canfield, H. Pan, D. Choi, X. Li and D. Reed, *Carbon Energy*, 2021, **3**, 473-481.
5. A. Salsabila, E. Prajatelistia, D. Y. Putro, A. N. Fahri, M. H. Alfaruqi and J. Kim, *J. Phys. Chem. Solids*, 2024, **188**, 111880.
6. S. Sarma Choudhury, N. Katiyar, R. Saha and S. Bhattacharya, *Sci. Rep.*, 2024, **14**, 1597.
7. Y. Li, X. Cui, J. Yan, Y. Zhang, E. Xie and J. Fu, *J. Colloid Interface Sci.*, 2023, **650**, 1605-1611.
8. V. Soundharrajan, B. Sambandam, S. Kim, S. Islam, J. Jo, S. Kim, V. Mathew, Y.-k. Sun and J. Kim, *Energy Storage Mater.*, 2020, **28**, 407-417.